PREDICTION OF CHANGES IN TOPOGRAPHY AND GRAIN SIZE OF SEABED MATERIALS USING THE BG MODEL

Yasuhito Noshi[1] and Takaaki Uda[2]

When beach changes occur owing to the imbalance of longshore sand transport, not only bathymetric changes but also grain size changes occur, having an impact on the coastal environment. With the increase in the anthropogenic impact, such changes have been observed on many coasts. Here, the bathymetric changes and changes in grain size of seabed materials were investigated on the basis of a numerical simulation using the BG model (a three-dimensional model for predicting beach changes based on Bagnold's concept), with northern Kujukuri Beach in Japan as the study area.

Keywords: Anthropogenic impact; beach changes; Kujukuri Beach; BG model; shoreline changes; grain size change

INTRODUCTION

When beach changes occur owing to the imbalance of longshore sand transport, not only bathymetric changes but also grain size changes occur, having an impact on the coastal environment. With the increase in the anthropogenic impact, such changes have been observed on many coasts. Thus, predictions of the bathymetric changes and changes in grain size of seabed materials are important from the engineering viewpoint. In this study, these issues are discussed on the basis of a numerical simulation, selecting northern Kujukuri Beach, as shown in Fig. 1, as the study area. Kujukuri Beach is a 60-km-long sandy beach and has been formed by the deposition of sand supplied from sea cliffs. In recent years, sand supply to this beach has markedly decreased mainly because of the measures taken to prevent the erosion of the sea cliffs. When beach changes are triggered by a decrease in longshore sand transport, fine sand moves much faster than coarse sand, resulting in a change in grain size of the seabed materials. Uda (2014) has predicted the beach changes of this coast using the BG model proposed by Serizawa et al. (2007), assuming that the seabed material is composed of single grain size. Here, we further predicted the beach changes of the coast with the seabed materials composed of two grain sizes using the BG model.

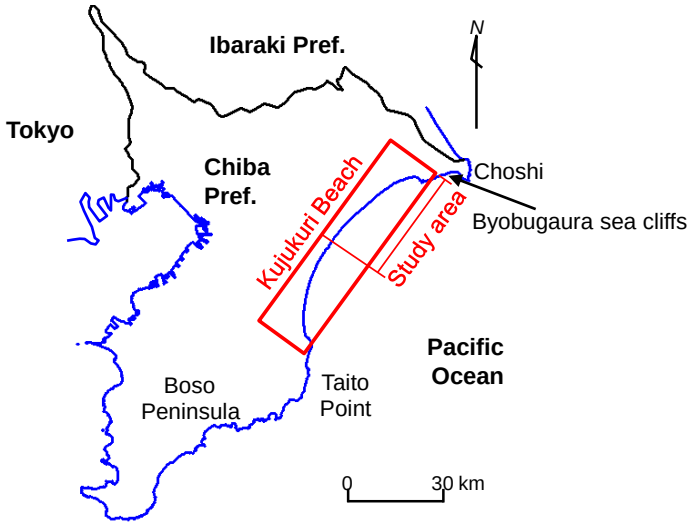

Figure 1. Location of Kujukuri Beach facing Pacific Ocean.

SHORELINE CHANGES

Figure 2 shows an aerial photograph of northern Kujukuri Beach in 2012. A gradually curved embayment shoreline extends from Iioka fishing port at the north end to Katagai fishing port. The

[1]Department of Oceanic Architecture & Engineering, College of Science & Technology, Nihon University, 7-24-1 Narashinodai, Funabashi, Chiba 274-8501, Japan
[2]Public Works Research Center, 1-6-4 Taito, Taito, Tokyo 110-0016, Japan

shoreline changes in this area between 1983 and 2012 were investigated using aerial photographs, as shown in Fig. 3 (Uda, 2014). The shoreline advance has been concentrated in the vicinity of Iioka fishing port and in the area northeast of Katagai fishing port. Except for the local shoreline advance around artificial structures, such as the detached breakwaters constructed between X = 6.2 and 7.2 km, the entire area between X = 5.0 and 20 km has eroded, the sandy beach has completely disappeared, and the seawall is now exposed to waves (Uda, 2014). The maximum shoreline advances were 160 and 130 m in the wave-shelter zone of Iioka fishing port and northeast of Katagai fishing port, respectively. In contrast, beach erosion was particularly severe in an area between X = 8.3 and 14.5 km, resulting in the complete disappearance of the foreshore in front of the seawall with a maximum shoreline recession of 70 m.

In 1947, Kujukuri Beach was a natural sandy beach, along which sand supplied from the Byobugaura sea cliffs northeast of the beach was transported by longshore sand transport toward the central part without any obstruction by artificial structures. By 2010, the Iioka fishing port breakwater had been extended together with the construction of 15 detached breakwaters downcoast (Uda, 2014). Owing to the extension of the south breakwater, westward longshore sand transport has been obstructed, and a large wave-shelter zone has formed west of the south breakwater, causing sand deposition. Also, sand was locally deposited at around X = 7 km because of the construction of three detached breakwaters, whereas the beach was severely eroded in between these sand deposition zones. Also, a large amount of sand has been deposited, as shown by the shoreline advance, because of the obstruction of longshore sand transport by the Katagai fishing port breakwater.

On northern Kujukuri Beach, artificial headlands (HLs) and detached breakwaters have been gradually constructed over time as a measure against beach erosion, as shown in Fig. 4. With the expansion of the eroded area, the area where countermeasures were taken also expanded downcoast, and twelve HLs had been constructed by 2010. In the calculation of wave field and beach changes, these records of the construction of the coastal facilities were taken into account.

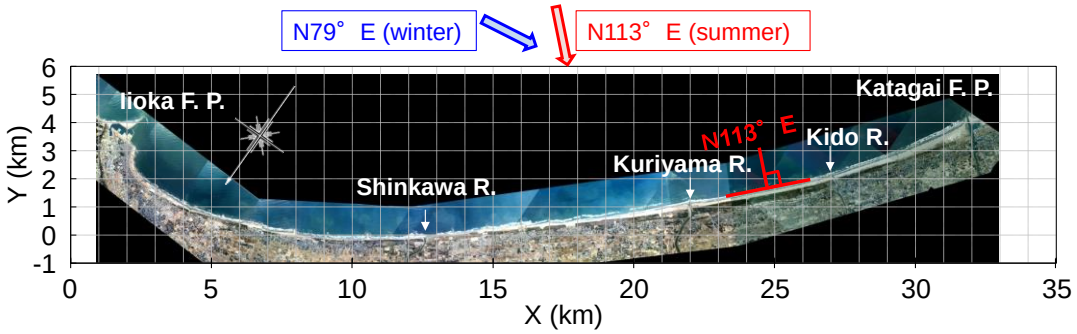

Figure 2. Aerial photograph of study area and calculation domain.

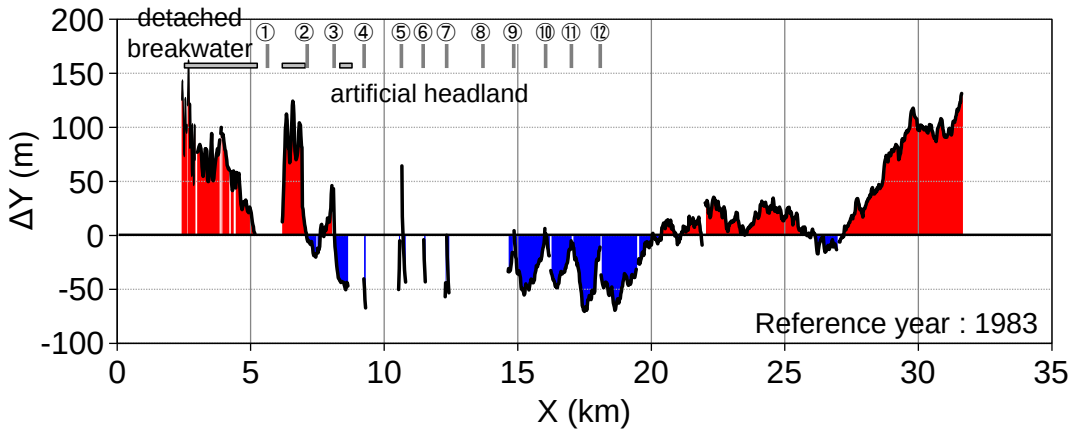

Figure 3. Shoreline changes until 2012 with reference to that in 1983 (Uda, 2014).

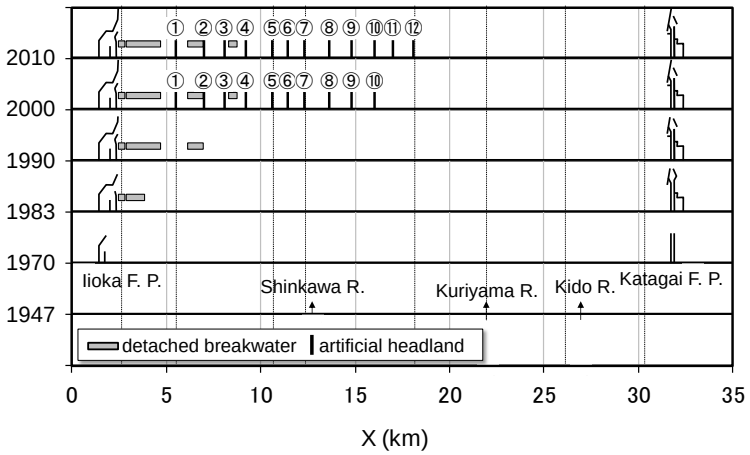

Figure 4. Construction history of coastal facilities.

NUMERICAL SIMULATION

Calculation of wave field

The calculation domain of the wave field is the rectangular zone between Iioka and Katagai fishing ports on northern Kujukuri Beach, as shown in Fig. 2. As the wave characteristics of the study area, the energy mean significant wave height is as low as 1.5 m (wave period of T = 11.3 s) in summer, whereas in winter, it increases to 2.0 m (T = 7.9 s), according to the results of wave observation offshore of Choshi (Tsuruoka et al., 2009). Therefore, the wave height ratio $K_r \bullet K_d$ and wave direction were independently calculated in summer and winter, given the wave incidence along the offshore boundary. The predominant wave direction in summer is from N113°E, whereas in winter, northerly wave incidence from N79°E prevails. Because the shoreline of the study area has a bay shape with a curvature, as shown in Fig. 2, longshore sand transport becomes 0 between X = 20 and 32 km, because the direction normal to the shoreline coincides with the wave direction of N113°E in summer in this area, whereas the angle between the normal to the shoreline and the wave direction is large between X = 2 and 20 km, resulting in strong longshore sand transport and marked beach changes in this area. In contrast, under the oblique wave incidence from N79°E in winter, an extensive wave-shelter zone is formed west of the Iioka fishing port breakwater, and longshore sand transport also approaches 0 in the wave-shelter zone. In other words, the effect of winter waves on beach changes in the wave-shelter zone of Iioka fishing port is negligible, but it increases with southwestward distance from the fishing port.

The shoreline of northern Kujukuri Beach has a bay shape with a large curvature, the effect of wave refraction is significant during the wave propagation between deep water and the breaker zone. Therefore, in the calculation of the wave field, the model proposed by Mase et al. (2001), in which both wave diffraction and refraction are taken into account, was employed. The bathymetry used for the calculation of the wave field was determined from the bathymetry measured in March 2011. We assumed that a flat seabed at 5 m depth extends to a zone shallower than -5 m only to evaluate the effect of wave diffraction around the structures.

Calculation of beach changes

The BG model proposed by Serizawa et al. (2007) was used for the calculation in which not only the beach changes but also changes in grain size can be calculated. The calculation domain is a 33-km-long coastline between Iioka and Katagai fishing ports, as shown in Fig. 2.

The depth of closure h_c necessary for the calculation was determined from Eq. (1), which is dependent on the wave height at a local point instead of a constant value, assuming a linear relationship between h_c and wave height H at a local point with a coefficient a.

$$h_c = aH \tag{1}$$

Here, h_c takes a maximum value of approximately 10 m near Katagai fishing port, as measured from the change in the longitudinal profile. When the energy mean wave height is used for H, the coefficient a becomes 5.0 from the relationship of Eq. (1), because the maximum wave height near Katagai fishing port in winter is given by approximately 2 m. Because h_c changes proportionally to the wave height H, h_c is small in the wave-shelter zone of Iioka fishing port, whereas it is larger near Katagai fishing port,

Table 1. Calculation conditions.

Calculation method	BG model (Serizawa et al., 2007)
Calculation area	Between Iioka and Katagai fishing ports on northern Kujukuri Beach
Calculation cases	Reproduction of topography in 2012 Case 1: Prediction of topography in 2062 Case 2: Beach nourishment of 5×10^5 m^3 using fine sand Case 3: Beach nourishment of 5×10^5 m^3 using coarse sand
Initial bathymetry	Reproduction calculation: Bathymetry produced from shoreline in 1983 assuming slope 1/50 Cases 1-3: Reproduced bathymetry in 2012
Grain size	Fine sand: 0.1 mm, Medium-size sand: 0.3 mm, coarse sand: 2.0 mm
Equilibrium slope	1/60 (d = 0.1mm), 1/50 (0.3 mm), 1/10 (2.0 mm)
Incident wave conditions	Breaker height H_b = 1.5 m, breaker angle α_b = 32.0° (N113°E) in summer Breaker height H_b = 2.0 m, Breaker angle α_b = 63.0° (N79°E) in winter
Water level	M.S.L. 0.0 m
Caluculation range of bathymetric changes	Depth of closure given by Eq. (1) and berm height h_R = 3.0 m
Boundary conditions	Left boundary: $1.4\times10^4$$m^3$/yr Right boundary: free
Coefficients of sand transport	Coefficient of sand transport A = 0.5 Coefficient of Ozasa and Brampton's (1980) term ζ = 1.62 Coefficient of cross-shore sand tranport relative to longshore sand transport K_y/K_x =0.7
Depth distribution of sand transport	Cubic equation by Uda and Kawano (1996)
Critical slope of falling sand	1/2 on land, 1/3 on seabed
Calculation range	X = 0.0 - 32.0 km in longshore direction, Y = 0.0 - 6.0 km cross-shore
Mesh size	ΔX = 50 m, ΔY = 20 m
Time intervals	Δt = 1hr
Total steps	8,760 steps/yr
Numerical simulation method	Explicit finite difference method

because there are no coastal structures. The maximum h_c values are 7.5 m in summer and 10 m in winter, because H_{max} in summer is 1.5 m.

Calculation conditions

The probability of occurrence of summer and winter waves is assumed to be equivalent considering the results measured at the Choshi wave observatory. The topography in 1983 was used as the initial topography. In the reproduction calculation, the construction history of coastal facilities up to 1990, 2000, and 2012, as shown in Fig. 4, was taken into account. The procedure of the installation of the coastal structures is the same as that described by Serizawa et al. (2003). Table 1 shows the calculation conditions.

In the model, the sandy beach is assumed to be composed of sand of the two grain sizes of 0.1 and 0.3 mm with equilibrium slopes of 1/60 and 1/50, respectively, on the basis of the field observation data. As the boundary condition, the longshore sand transport at the north end was assumed to be 1.4×10^4 m^3/yr, estimated between 1985 and 2005 from the annual rate of accumulation of sand east of the Iioka fishing port breakwater. At the south end of the calculation domain, a free boundary was set, resulting in a rate of longshore sand transport of approximately 7.0×10^4 m^3/yr, which was equal to a simulation result for southern Kujukuri Beach (San-nami et al., 2011). The grain size composition of the sand was assumed to be 65% for fine sand and 35% for medium-size sand at the upcoast boundary, and at the downcoast boundary, the same grain size composition was employed.

RESULTS

The wave fields in summer and winter employed for the calculation of beach changes between 2000 and 2012, for example, are shown in Figs. 5 and 6, respectively. The distribution of $K_r \bullet K_d$ in winter in the longshore direction is markedly different from that in summer, because the wave-sheltering effect of the Iioka fishing port breakwater against waves with easterly incidence is greater in winter than in summer. Regarding the wave direction, waves are incident toward the wave-shelter zone both in summer and winter owing to the wave-sheltering effect of the Iioka fishing port breakwater. Because the Iioka fishing port breakwater and artificial headlands have been constructed on the coast

over time, the wave fields in summer and winter employed for the calculation between 1983 and 1990, and between 1990 and 2000 were also calculated, similarly to those shown in Figs. 5 and 6.

Figure 7 shows the initial bathymetry in 1983 and the distribution of the mean grain size of bed materials. The bed material is assumed to be composed of sand of mixed grain sizes of 0.1 and 0.3 mm, and the grain size composition of the sand was assumed to be 65% for fine sand and 35% for medium-size sand on the basis of the average of the measured data, which are uniformly distributed. Figure 8 shows the calculated bathymetry in 2012, bathymetric changes with reference to that in 1990 and the distribution of the mean grain size of seabed materials. It is clear that the beach between X =7.5 and 20.3 km was severely eroded, resulting in the shoreline recession with local accretion and erosion immediately north and downcoast of the artificial headlands, respectively. In contrast, accretion occurred downcoast of X = 22 km.

Figures 9 and 10 show the detailed bathymetry and grain size distribution in rectangular areas A and B in Fig. 8. In the area between X = 17 and 20 km, where the beach was eroded, the grain size of the seabed materials increased, except the upcoast of the artificial headland where the local accumulation of fine materials occurred, whereas near Katagai fishing port, fine sand was deposited because of the selective movement of fine sand owing to the southwestward longshore sand transport.

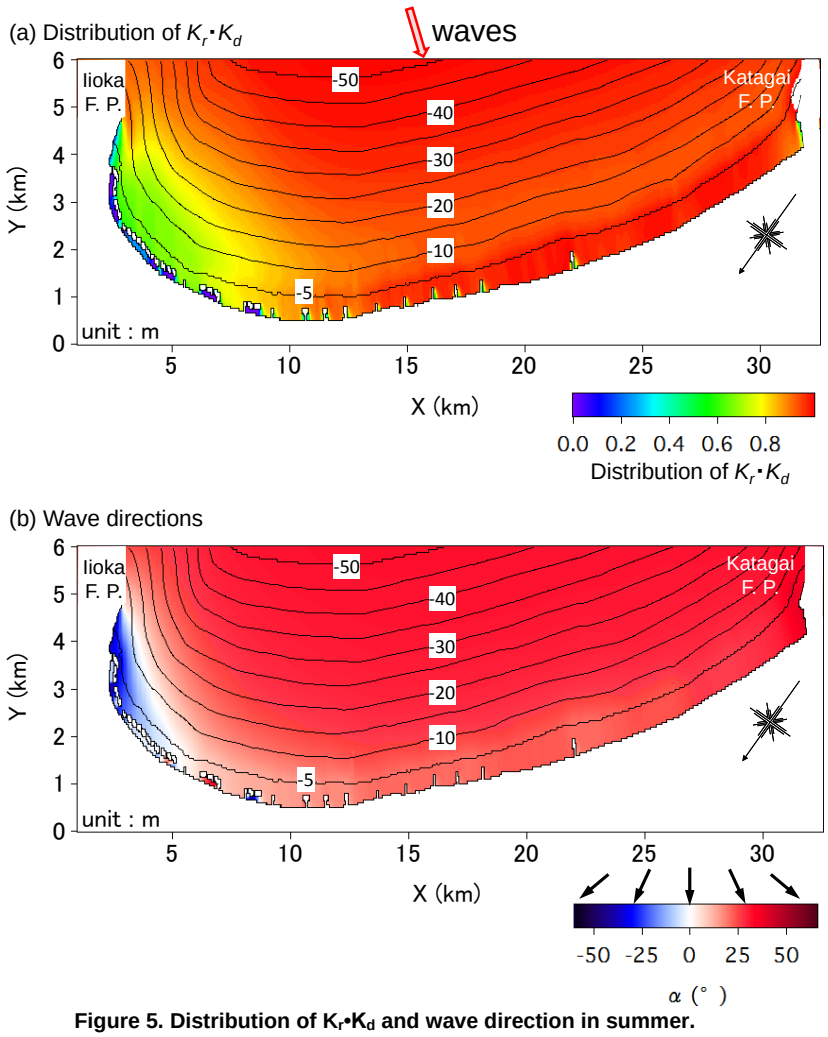

Figure 5. Distribution of K_r･K_d and wave direction in summer.

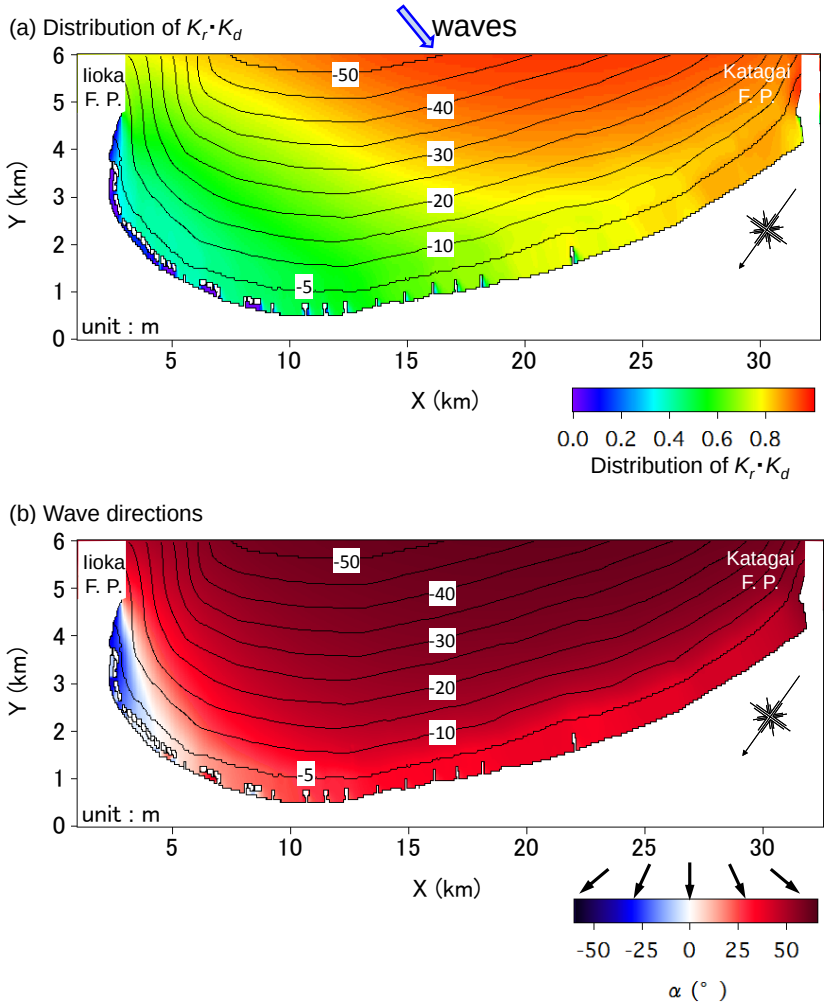

Figure 6. Distribution of K_r•K_d and wave direction in winter.

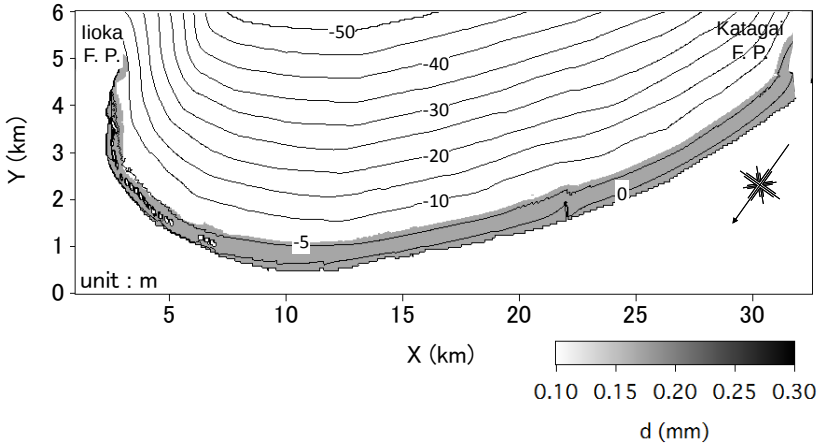

Figure 7. Initial bathymetry and distribution of mean grain size in 1983.

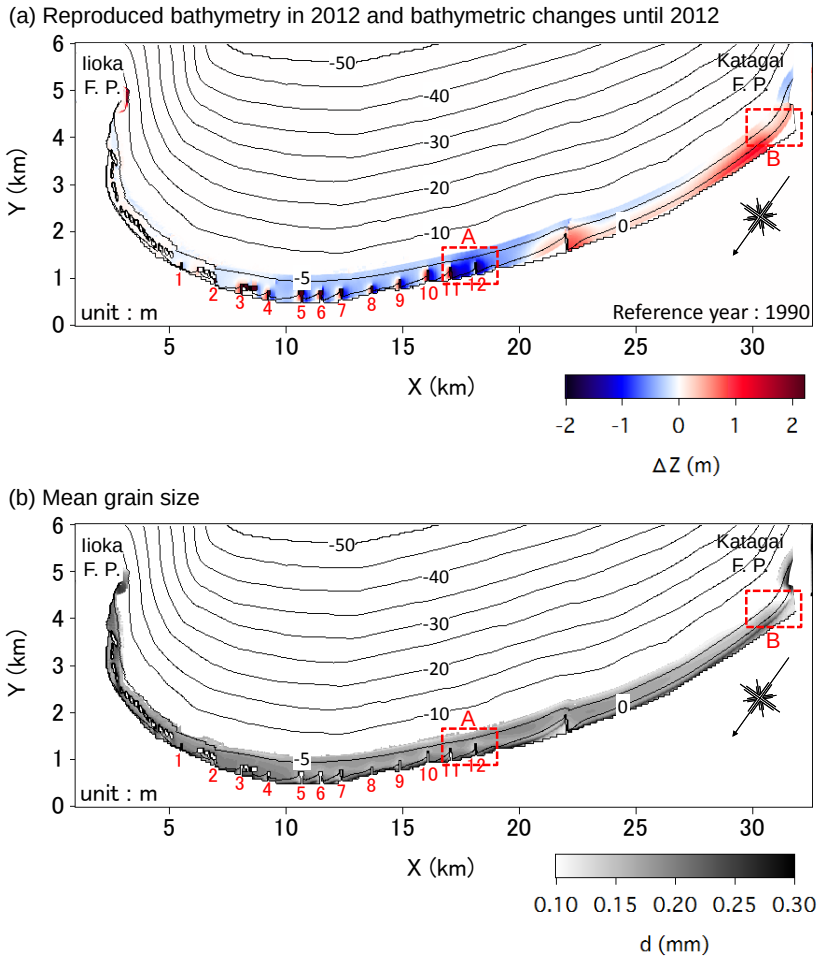

Figure 8. Reproduced bathymetry in 2012, bathymetric changes with reference to that in 1990 and distribution of mean grain size of seabed materials.

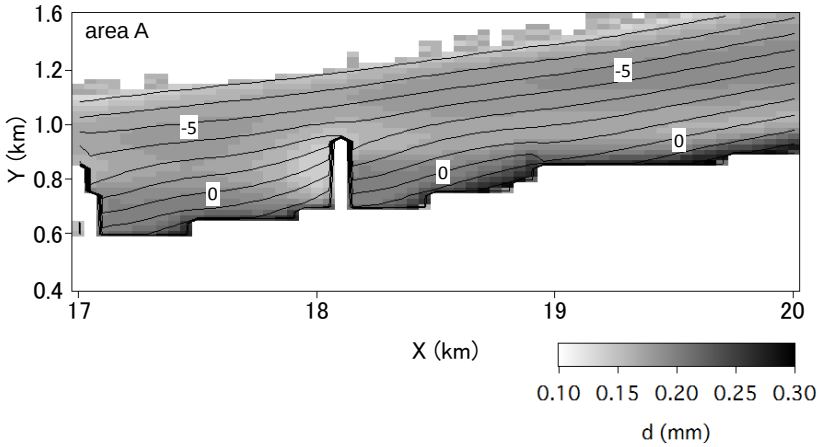

Figure 9. Bathymetry and grain size distribution in rectangular area A.

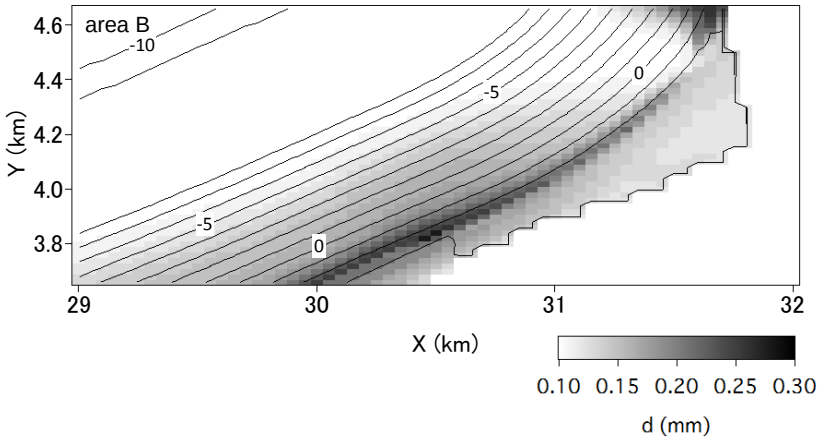

Figure 10. Bathymetry and grain size distribution in rectangular area B.

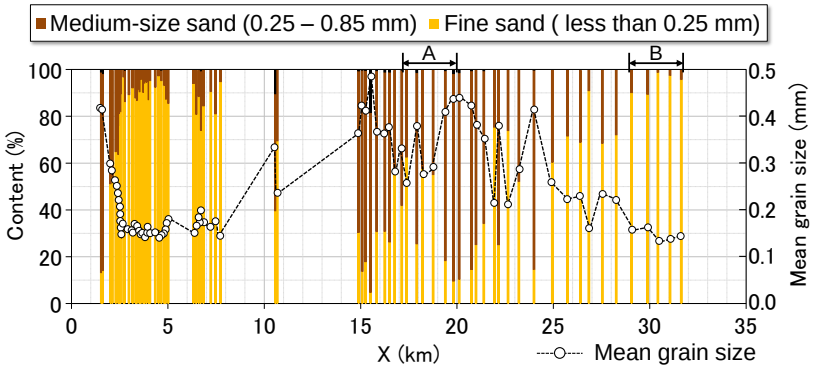

Figure 11. Longshore distribution of content and mean grain size of foreshore materials measured on November 18, 2011.

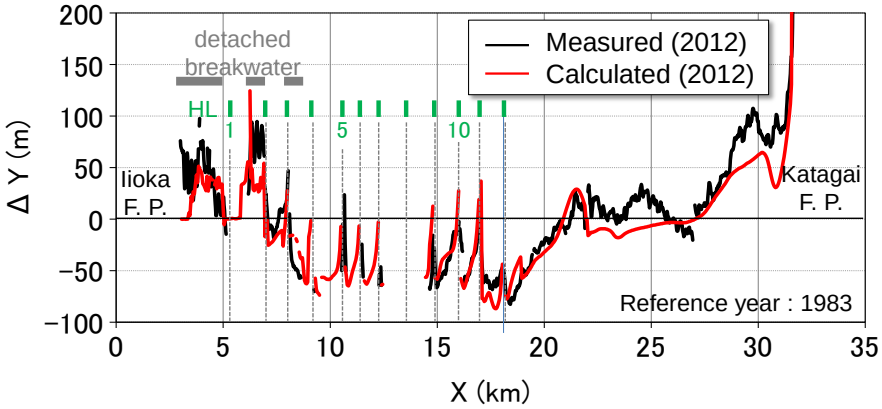

Figure 12. Shoreline changes up to 2012 with reference to that in 1983.

Figure 11 shows the longshore distribution of the content and mean grain size of foreshore materials sampled along the shoreline on November 18, 2011. The measured longshore distribution shown in Fig. 11 and the calculated distribution shown in Fig. 10 are in good agreement. The calculated shoreline changes between 1983 and 2012 are shown in Fig. 12. Marked shoreline changes were triggered by the construction of the detached breakwaters and the artificial headlands. Behind the detached breakwater, further sand deposition occurred, whereas the shoreline receded between X =7.5 and 20.3 km. Also, the shoreline advanced on the northeast side of Katagai fishing port. The calculated and measured shoreline changes are in good agreement.

Finally, it was concluded that the beach has been eroded on northern Kujukuri Beach owing to (1) the decrease in sand supply from Byobugaura sea cliffs, (2) the disruption of longshore sand supply by

the Iioka fishing port beakwater and detached breakwaters constructed downcoast of the fishing port, and (3) the discharge of sand by longshore sand transport turning around the tip of Katagai fishing port at the downcoast boundary. Furthermore, grain size sorting by longshore sand transport occurred, resulting in an increase (decrease) in grain size in the eroded (accreted) area. Since the grain size deposited around Katagai fishing port was small with high mobility, sand was easily transported downcoast.

EFFECT OF BEACH NOURISHMENT

The results of the reproduction calculation show that the beach erosion is severe in an area between HL Nos. 8 and 12 located in the central part of northern Kujukuri Beach. Therefore, the effect of beach nourishment using fine and coarse sand was investigated as a measure for restoring the foreshore in this area. First, in Case 1, beach changes until 2062 with no measures were predicted, given the reproduced bathymetry in 2012 as the initial bathymetry, and assuming the completion of the construction of all the artificial headland Nos. 1-12.

Figure 13 shows the predicted bathymetry in 2062 and bathymetric changes with reference to the bathymetry in 2012. It is realized that erosion becomes severe in the entire area except for the immediate vicinity of the northeast side of each HL because of the discharge of sand from the study area by southwestward longshore sand transport. Figure 14 shows the detailed bathymetric changes in the vicinity of the HLs, as shown in the rectangular zone in Fig. 13. Sand was deposited only on the northeast side of the HLs by the blockage of southwestward longshore sand transport by the HLs, resulting in an average increase of 0.7 m in water depth. This is because part of the longshore sand transport discharged downcoast while turning around the tip of the HLs, because the water depth at the tip of the HLs is smaller than the depth of closure. Meandering contour lines offshore of the HLs also show the development of southwestward longshore sand transport.

Figure 15 shows the beach width measured from the seawall in 2012. Although the foreshore had completely disappeared between X = 7.1 and 19.0 km by 2012, the eroded area further expanded downcoast up to X = 20.5 km, implying the necessity of some measure against beach erosion.

In Case 2, the effect of beach nourishment using fine sand of 5.0×10^5 m^3, for example, to recover the foreshore was investigated. Figures 16 and 17 show the initial bathymetry in Case 2 with the nourishment area between HL Nos. 7 and 12. Then, the predicted bathymetry in 2062 in Case 2 and bathymetric changes with reference to the bathymetry in Case 1 are shown in Fig. 18. The nourishment sand was quickly transported southwestward, leaving the upcoast eroded up to the level before the nourishment, and resulting in no effect of beach nourishment. Figure 19 shows the change in beach width measured from the seawall in 2012. The foreshore recovered slightly in an area between HL Nos. 10 and 11, and on the north side of HL No. 12, but the effect of beach nourishment was indistinct, implying the inadequency of beach nourishment using fine sand as a measure against beach erosion. The reason is that fine sand was easily transported away by the predominant longshore sand transport.

In Case 3, the effect of beach nourishment using coarse sand was investigated keeping the nourishment volume constant as 5.0×10^5 m^3, similar to Case 2, and selecting the same nourishment area, as shown in Fig. 17. The predicted bathymetry in 2062 and the bathymetric changes with reference to that in Case 1 are shown in Fig. 20. Coarse sand was intensively deposited on the foreshore between the HLs without offshore dispersion, resulting in an average increase of 0.7 m in the ground elevation. Figure 21 shows the change in beach width with reference to the seawall in 2012. The recovery of the foreshore between HL Nos. 7 and 12 is clear.

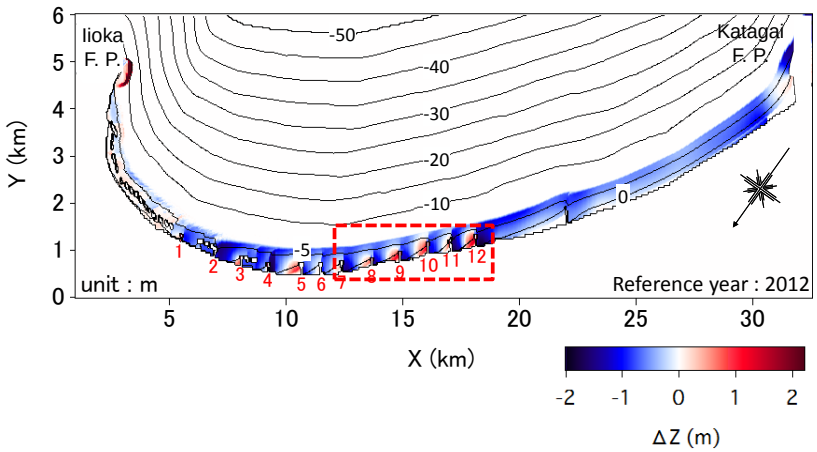

Figure 13. Predicted bathymetry in 2062 and bathymetric changes with reference to that in 2012.

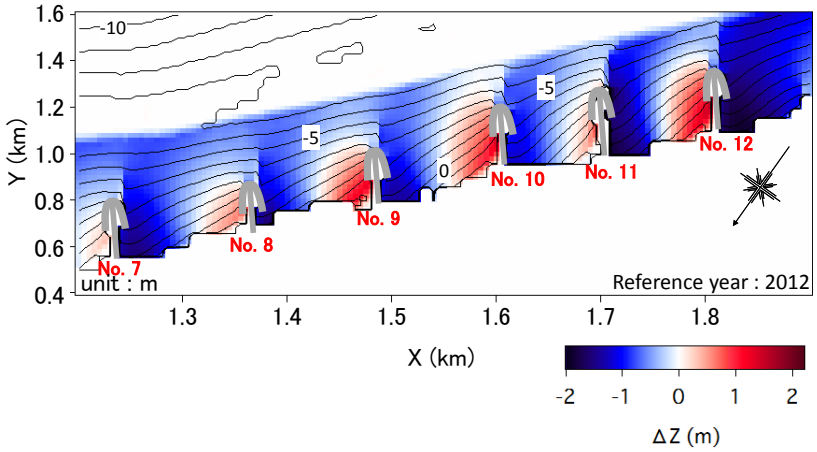

Figure 14. Bathymetric changes up to 2062 around HLs.

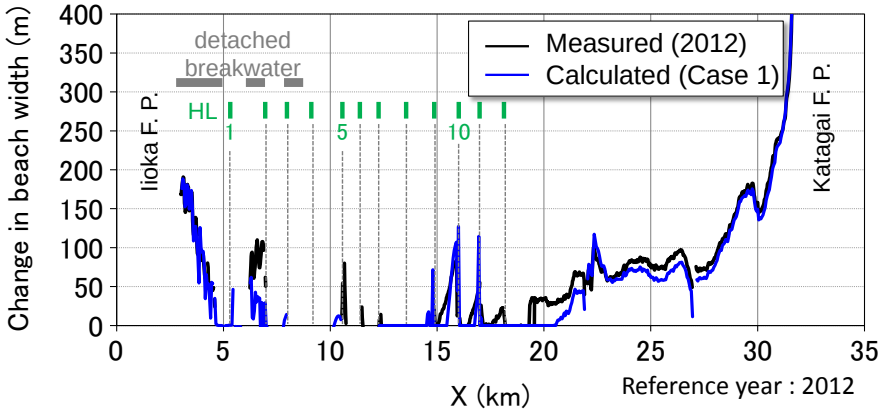

Figure 15. Change in beach width in Case 1.

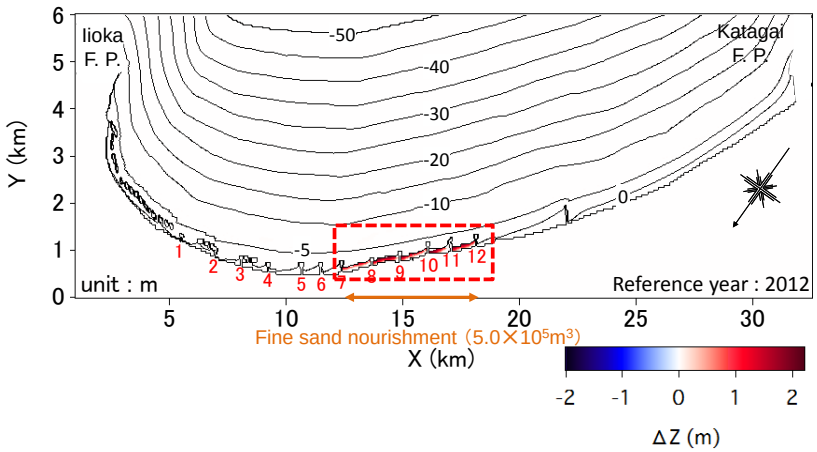

Figure 16. Beach nourishment area (Case 2).

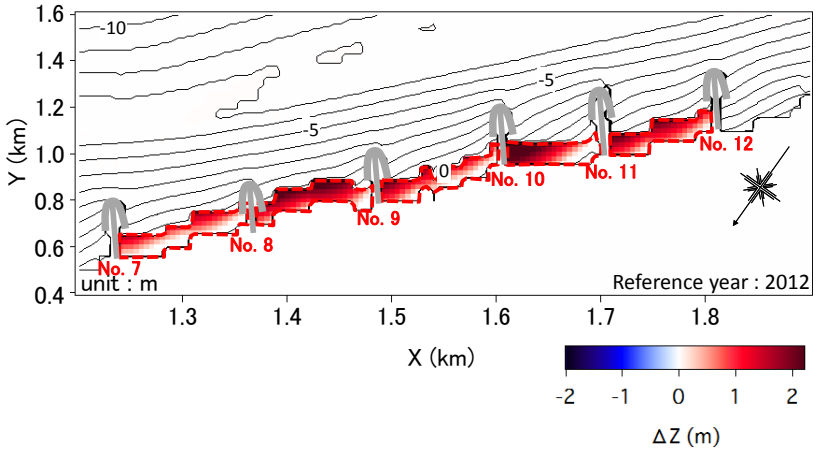

Figure 17. Detailed topography in nourishment area (Case 2).

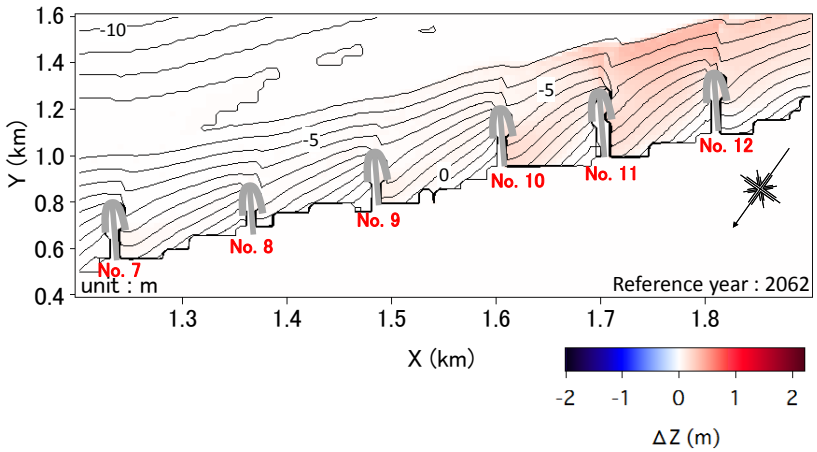

Figure 18. Bathymetric changes in Case 2 with reference to that in Case 1.

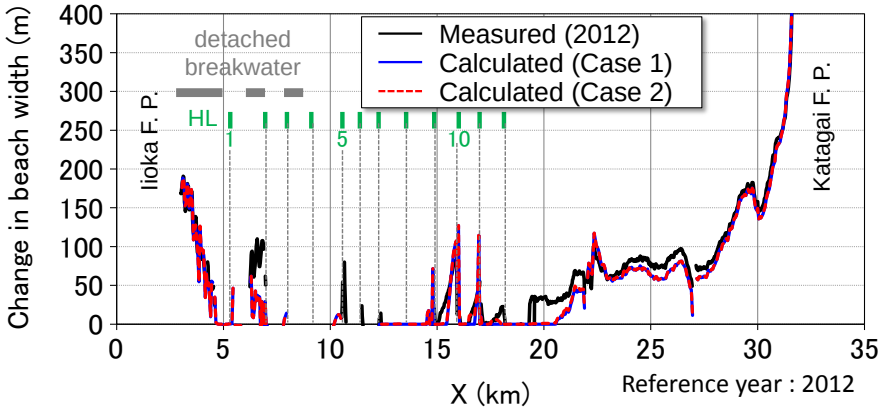

Figure 19. Change in beach width (Case 2).

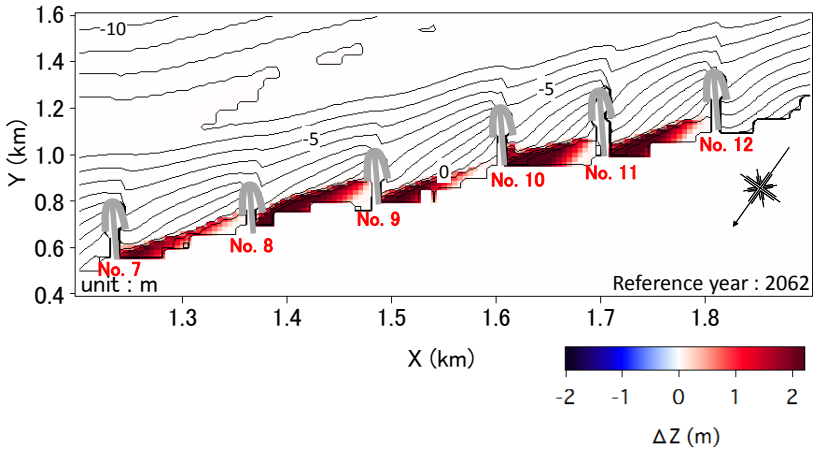

Figure 20. Bathymetric changes in Case 3 with reference to that in Case 1.

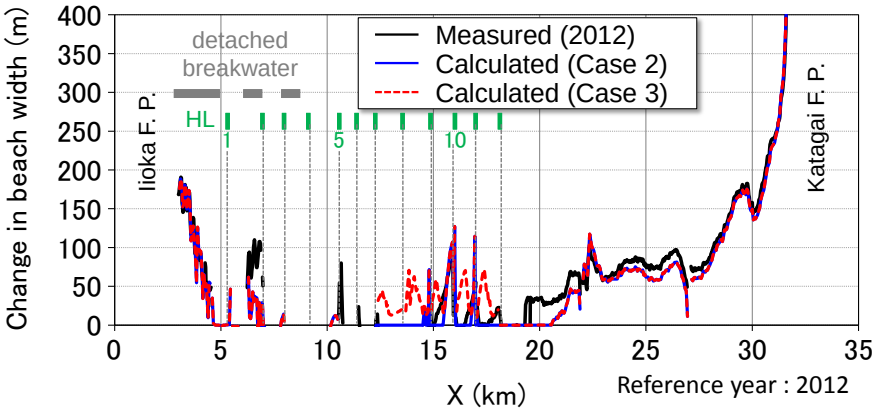

Figure 21. Change in beach width (Case 3).

CONCLUSIONS

The bathymetric and grain size changes on northern Kujukuri Beach were reproduced using the BG model. It was concluded that the beach changes in the study area were triggered by the imbalance of longshore sand transport and the selective movement of fine sand. With time, not only shoreline recession but also changes in grain size of the seabed materials occur, and such changes can be successfully predicted using the BG model. By numerical simulation, the effectivenes of beach nourishment using coarse sand was also demonstrated. On the other hand, beach nourishment using coarse sand is considered to be inferior to that using fine sand from the viewpoint of coastal utilization such as bathing in summer. However, fine sand could be deposited on a basement of coarse sand by

shoreward sand transport, which occurs under calm wave conditions in summer, reducing the damage to marine sports. Further studies are necessary to investgate these points.

REFERENCES

Mase, H., Oki, K., Takayama, T. and Sakai, T. 2001. Phase averaging model for multi-directional random wave transformation by high order upwind difference scheme, *J. JSCE*, No. 684, II-56, pp. 57-68. (in Japanese)

Ozasa, H., and Brampton, A. H. 1980. Model for predicting the shoreline evolution of beaches backed by seawalls, Coastal Eng., Vol. 4, pp. 47-64.

San-nami, T., Furuike, K., Uda, T. and Serizawa, M. 2011. Formation of an arc-shaped accretive shoreline downcoast of sea cliffs and prediction of deformation, *Coastal Sediments '11*, pp. 1243-1256.

Serizawa, M., Uda, T., San-nami, T., Furuike, K. and Kumada, T. 2003. Improvement of contour line change model in terms of stabilization mechanism of longitudinal profile, *Coastal Sediments '03*, pp. 1-15.

Serizawa, M., Uda, T., San-nami, T., Furuike, K., Ishikawa, T. and Kumada, K. 2007. Model for predicting beach changes on coast with sand of mixed grain size based on Bagnold's concept, *Coastal Sediments '07*, pp. 314-326.

Tsuruoka, H., Uda, T., Serizawa, M., Furuike, K., Fukumoto, T., Hoshigami, Y. and Miyahara, S. 2009. Investigation of effect of offshore nourishment and continuous sand supply on south Kujukuri Beach, *J. JSCE*, Vol. 56, pp. 711-715. (in Japanese)

Uda, T. and Kawano, S. 1996. Development of contour-line change model for predicting beach changes, *Proc. JSCE*, No.539/II-35, pp. 121-139, 1996. (in Japanese)

Uda, T. 2014. Downcoast erosion triggered by exhaustion of sand supply from sea cliffs - an example of northern Kujukuri Beach in Japan, Chapter 6, pp. 121-146, In *'Beaches'*, M. Cessa ed., Nova publishers, New York, USA.
https://www.novapublishers.com/catalog/product_info.php?products_id=50372